Mechanisms of fever-induced QT prolongation and torsades de pointes in patients with *KCNH2* mutation

Keisuke Usuda [1], Kenshi Hayashi [1]*, Tadashi Nakajima [2], Yasutaka Kurata[3], Shihe Cui[1], Takashi Kusayama [1], Toyonobu Tsuda[1], Hayato Tada [1], Takeshi Kato [1], Kenji Sakata[1], Soichiro Usui [1], Noboru Fujino [1], Yoshihiro Tanaka [1,4], Yoshiaki Kaneko[2], Masahiko Kurabayashi [2], Shoichi Tange [5], Takekatsu Saito [6], Kunio Ohta [6], Masakazu Yamagishi[7], and Masayuki Takamura [1]

[1]Department of Cardiovascular Medicine, Kanazawa University Graduate School of Medical Sciences, 13-1, Takara-machi, Kanazawa Ishikawa 920-8641, Japan; [2]Department of Cardiovascular Medicine, Gunma University Graduate School of Medicine, Maebashi, Japan; [3]Department of Physiology, Kanazawa Medical University, Uchinada, Japan; [4]Department of Preventive Medicine Northwestern University, Feinberg School of Medicine, Chicago, IL, USA; [5]Department of Cardiovascular Medicine, Maebashi Red Cross Hospital, Maebashi, Japan; [6]Department of Pediatrics, Kanazawa University, Kanazawa, Japan; and [7]Osaka University of Human Sciences, Osaka, Japan

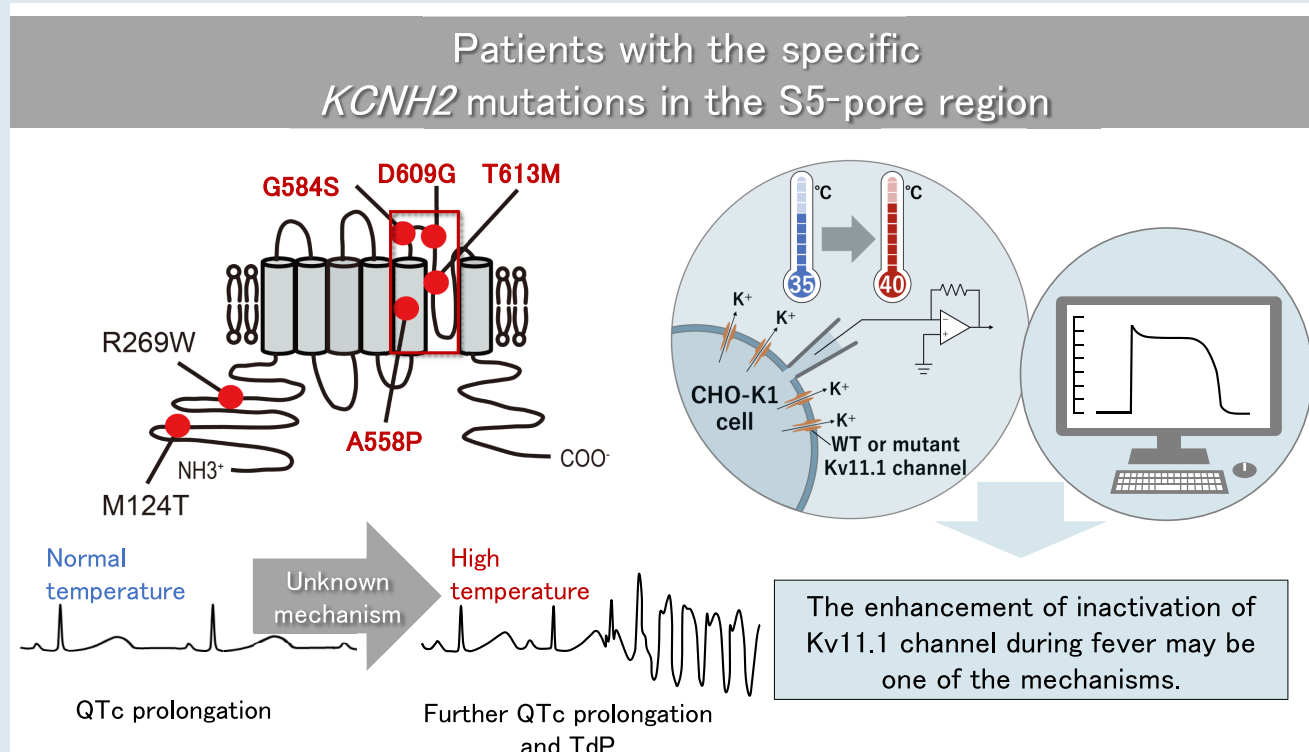|	
Aims	Patients with particular mutations of type-2 long QT syndrome (LQT2) are at an increased risk for malignant arrhythmia during fever. This study aimed to determine the mechanism by which *KCNH2* mutations cause fever-induced QT prolongation and torsades de pointes (TdP).
Methods and results	We evaluated three *KCNH2* mutations, G584S, D609G, and T613M, in the Kv11.1 S5-pore region, identified in patients with marked QT prolongation and TdP during fever. We also evaluated *KCNH2* M124T and R269W, which are not associated with fever-induced QT prolongation. We characterized the temperature-dependent changes in the electrophysiological properties of the mutant Kv11.1 channels by patch-clamp recording and computer simulation. The average tail current densities (TCDs) at 35°C for G584S, WT+D609G, and WT+T613M were significantly smaller and less increased with rising temperature from 35°C to 40°C than those for WT, M124T, and R269W. The ratios of the TCDs at 40°C to 35°C for G584S, WT+D609G, and WT+T613M were significantly smaller than for WT, M124T, and R269W. The voltage dependence of the steady-state inactivation curve for WT, M124T, and R269W showed a significant positive shift with increasing temperature; however, that for G584S, WT+D609G, and WT+T613M showed no significant change. Computer simulation demonstrated that G584S, WT+D609G, and WT+T613M caused prolonged action potential durations and early afterdepolarization formation at 40°C.
Conclusion	These findings indicate that *KCNH2* G584S, D609G, and T613M in the S5-pore region reduce the temperature-dependent increase in TCDs through an enhanced inactivation, resulting in QT prolongation and TdP at a febrile state in patients with LQT2.

Graphical Abstract

Patients with the specific *KCNH2* mutations in the S5-pore region

The enhancement of inactivation of Kv11.1 channel during fever may be one of the mechanisms.

What's New?

- *KCNH2* G584S, D609G, and T613M in the Kv11.1 S5-pore region, identified in the LQT2 patients with fever-induced QT prolongation and torsades de pointes, reduced the temperature-dependent increase in tail current densities (TCDs) of Kv11.1 channel through the reduced temperature-dependent depolarizing shift of steady-state inactivation.
- In contrast, *KCNH2* wild-type and M124T and R269W in the Kv11.1 N-terminus, which were identified in the patients with long QT syndrome, increased TCDs with increasing temperature.
- Some patients with specific *KCNH2* mutations in the S5-pore region may develop QT prolongation and life-threatening arrhythmias in the febrile state due to the enhanced inactivation of Kv11.1 channel.

Introduction

Long QT syndrome (LQTS) is an inherited cardiac disorder characterized by delayed repolarization of ventricular action potentials (APs) and malignant arrhythmia, which may lead to syncope, cardiac arrest, and sudden death.[1,2] Genetic studies have identified 17 forms of congenital LQTS caused by mutations in genes encoding cardiac ion channels or ion channel modulators, including membrane adapters.[3] The acquired form of LQTS is more common than the congenital form. Risk factors for acquired LQTS include drugs administered for non-cardiac conditions, use of over-the-counter drugs, hypokalemia, bradycardia, and genetic variations in ion channel genes.[4,5]

Fever has rarely been recognized as a trigger for cardiac events in LQTS. Previous studies showed that hyperthermia resulted in a temperature-dependent decrease in AP amplitude and AP duration at 90%

repolarization in guinea pig papillary muscles.[6,7] In normal subjects, rate-corrected QT interval (QTc) duration decreased with increasing body temperature.[8] Whole-cell patch clamp experiments showed that current densities of the repolarizing delayed rectifier K^+ currents[9] and the depolarizing cardiac Na^+ and Ca^{2+} currents[10] increase at a higher temperature. The balance between depolarizing and repolarizing currents may favor repolarization during fever in normal subjects.[6]

Few studies have reported QT prolongation and torsades de pointes (TdP) that were triggered by fever in patients with *KCNH2* mutations.[8,11,12] *KCNH2* A558P was identified in patients with type-2 LQTS (LQT2) who showed prolonged QTc and TdP with fever (39.7°C).[8] *KCNH2* T613M was identified in a young Japanese woman who developed QT prolongation and TdP triggered by fever (38°C or higher).[11] Additionally, we identified two patients who presented QT prolongation and TdP during fever and harbored *KCNH2* G584S[12] or D609G mutation.[13] Interestingly, all these mutations are located in the Kv11.1 S5-pore region, which may be related to the underlying mechanism of fever-induced QT prolongation and TdP.

One study has reported the mechanisms of fever-induced QT prolongation and TdP in patients with the *KCNH2* A558P mutation;[8] however, there is insufficient data on the biochemical and biophysical mechanisms of other *KCNH2* mutations. In this study, we sought to characterize the temperature-dependent changes in the electrophysiological properties of *KCNH2* G584S, D609G, and T613M in the S5-pore region to elucidate the mechanisms of fever-induced QT prolongation and TdP.

Methods

An expanded Methods section is available in the *Supplementary Material* online.

DNA isolation and mutation analysis

Genomic DNA was extracted from peripheral blood leukocytes using standard methods. All exons of the *KCNQ1*, *KCNH2*, *SCN5A*, *KCNE1*, *KCNE2*, and *KCNJ2* genes were sequenced.

This study followed the principles outlined in the Declaration of Helsinki and was approved by the Ethics Committee of Medical Research at Kanazawa University, Graduate School of Medical Science and Gunma University, Graduate School of Medical Science. All study patients provided written informed consent before registration.

Plasmid constructs and transfection

The hERG (*KCNH2*) cDNA in the pSI vector was kindly provided by Dr. Sabina Kupershmidt. Mutant cDNAs were constructed. CHO-K1 cells were transiently transfected with wild-type (WT) cDNA alone (1.0 µg), mutant (MT) cDNA alone (1.0 µg), or WT and MT in a 1:1 molar ratio (0.5 µg each), using FuGene 6 (Promega, WI, USA). Cells displaying green fluorescence 48–72 h after transfection were subjected to electrophysiological analysis.

Electrophysiology and data analysis

Potassium currents were studied using the whole-cell patch clamp technique at room temperature (25°C), physiological temperature (35°C), and high temperature (40°C). Electrode resistance ranged from 2 to 4 MΩ for potassium channel recordings when the glass electrodes were filled with the pipette solution. The voltage clamp protocols have been described previously[14] and are available in the figures. The voltage dependence of the potassium current activation was measured for each cell. The amplitudes of the tail currents were normalized to [0, 1], and the normalized tail-current amplitudes (I_{tail}) were plotted against the test potential and fitted using a Boltzmann function with the following form: $I_{tail} = 1 / \{1 + \exp[(V_{1/2} - V_t) / k]\}$, where V_t is the test potential, $V_{1/2}$ is the half-maximum voltage, and k is the slope factor. Steady-state inactivation of the Kv11.1 channels was analyzed, as described previously.[14] For extremely negative voltages, the rapid closing that occurred during the brief hyperpolarizing step was corrected.[15] The corrected steady-state inactivation curves were fitted with the Boltzmann function. All results at 35°C and 40°C were obtained from paired experiments, i.e. we measured the potassium current consecutively at 35°C and then re-measured it at 40°C for the same sample.

Computer simulations of human ventricular action potentials for wild-type and each mutant *KCNH2*

We simulated early afterdepolarization (EAD) generations in LQT2 cardiomyocytes using a mathematical model of human ventricular myocytes developed by Kurata *et al.*[16] A mid-myocardial (M) cell version of the model was developed based on transmural heterogeneity in densities of sarcolemmal ion channels and intracellular Ca^{2+} dynamics, as summarized by O'Hara *et al.*[17] and in Supplementary material online, Table S1. We employed the M cell version because it has high I_{CaL} and low I_{Kr} and I_{Ks}, thus being much more vulnerable to EAD formation than the endocardial and epicardial versions. Action potentials were elicited by 1-ms stimuli of 60 pA/pF at 1 Hz. For simulating the febrile state as a trigger for EADs and TdP in LQT2, parameters describing the maximum conductance and gating kinetics of the rapidly activating delayed rectifier K$^+$ channel current (I_{Kr}) were modified based on the temperature-dependent behaviors of the WT and mutants observed in this study.

The Q10 values for the maximum conductance and activation/inactivation rates of the WT and mutant Kv11.1 channels, as well as those of each mutant's Kv11.1 channels relative to those of the WT, are specified in Supplementary material online, Table S2. The activation and inactivation curves for the Kv11.1 channels were assumed to shift linearly, depending on the temperature between 35°C and 40°C. Temperature-dependent behaviors of the L-type Ca^{2+} channel current (I_{CaL}) and the inward-rectifier K$^+$ channel current (I_{K1}) were also formulated using the Q10 of 2.3 and 1.5, respectively, according to the report by Kiyosue *et al.*[6]

Statistical analysis

We checked the normality of the data on the parameters of tail current and Kv11.1 channel kinetics using QQ plots and Shapiro–Wilk test. Pooled electrophysiological data were expressed as mean ± standard error. Two-tailed Student's *t*-test was used to compare the two groups. Paired *t*-test was used to compare the means of two groups in the case of two samples that are correlated. One-way analysis of variance (ANOVA), followed by *post hoc* Tukey's test, was used to analyze data with equal variance among three or more groups. Two-way ANOVA, followed by *post hoc* Tukey's test, was used to analyze data regarding the rate of channel inactivation between the WT and mutant channels. A value of *P* < 0.05 was considered statistically significant. Statistical analysis was performed using Origin 9.8 (OriginLab, Northampton, MA, USA).

Results

Clinical characteristics and gene analyses

Case 1 is a 47-year-old woman who experienced syncope caused by TdP during fever.[12] She was previously diagnosed with drug-induced LQTS caused by antidepressant use (fluvoxamine and trazodone) at age 40, discontinuing the drug use thereafter. At age 47, she experienced marked QT prolongation (QTc = 563 ms) and TdP during an outpatient visit for moderate grade fever (38.5°C) due to pyelonephritis. *Figure 1A*, left and *Figure 1B* shows QT prolongation and TdP on admission. Then, she had a mild prolonged QTc interval of 444 ms after her temperature had gone down (*Figure 1A*, right).

Case 2 involved a 2-year-old boy who was diagnosed with bradycardia at birth. At age 2, he was prescribed clarithromycin for acute bronchitis without fever (37.3°C) at a hospital. Three days later, he returned to the hospital because of a moderate grade fever (39°C). Electrocardiography performed in the emergency room revealed marked QT prolongation (QTc = 566 ms, *Figure 1C*, left) and TdP (*Figure 1D*). Even after his temperature decreased, he still had a prolonged QTc interval of 532 ms (*Figure 1C*, right).

We identified a *KCNH2* G584S mutation from Case 1[12] and a *KCNH2* D609G mutation and a *KCNQ1* D611Y mutation from Case 2.[13] We also evaluated *KCNH2* T613M, which was previously reported.[11] The patient with *KCNH2* T613M was a 25-year-old female diagnosed with LQTS at age 8. At age 25, she experienced an episode of QT prolongation (QTc = 695 ms) and TdP during low-grade fever (38°C or higher) due to an infection of a central venous catheter inserted for treatment of adult-onset type 2 citrullinemia. After her temperature had gone down, she still had a prolonged QTc interval of 600 ms.

These three *KCNH2* mutations were located in the Kv11.1 S5-pore region (*Figure 1E*). We also evaluated two other mutations, *KCNH2* M124T and R269W, which are distinct from the Kv11.1 S5-pore region (*Figure 1E*). M124T was identified from a 59-year-old woman with drug-induced LQTS and R269W in a 47-year-old woman with LQTS.[5] They had never experienced syncope during fever. All patients with *KCNH2* G584S, D609G, T613M, M124T, and R269W, and *KCNQ1* D611Y were heterozygous.

Comparisons of the cellular electrophysiological properties of *KCNH2* mutants at 25°C

Whole-cell voltage clamp measurements were performed using cultured CHO-K1 cells that were transiently expressing Kv11.1 WT or mutants at 25°C to define the basal functional effect of the five *KCNH2* variants. Voltage clamp recordings from the cells expressing M124T alone, R269W alone, or G584S alone demonstrated functional channel currents with relatively small amplitudes. In contrast, those expressing D609G alone or T613M alone showed no functional channel currents (see Supplementary material online, Figure S1A). Co-expression of G584S, D609G, or T613M with WT resulted in significant tail current densities (TCDs), which were less than half of the control current observed with the expression of WT alone (see Supplementary material online, *Figures*
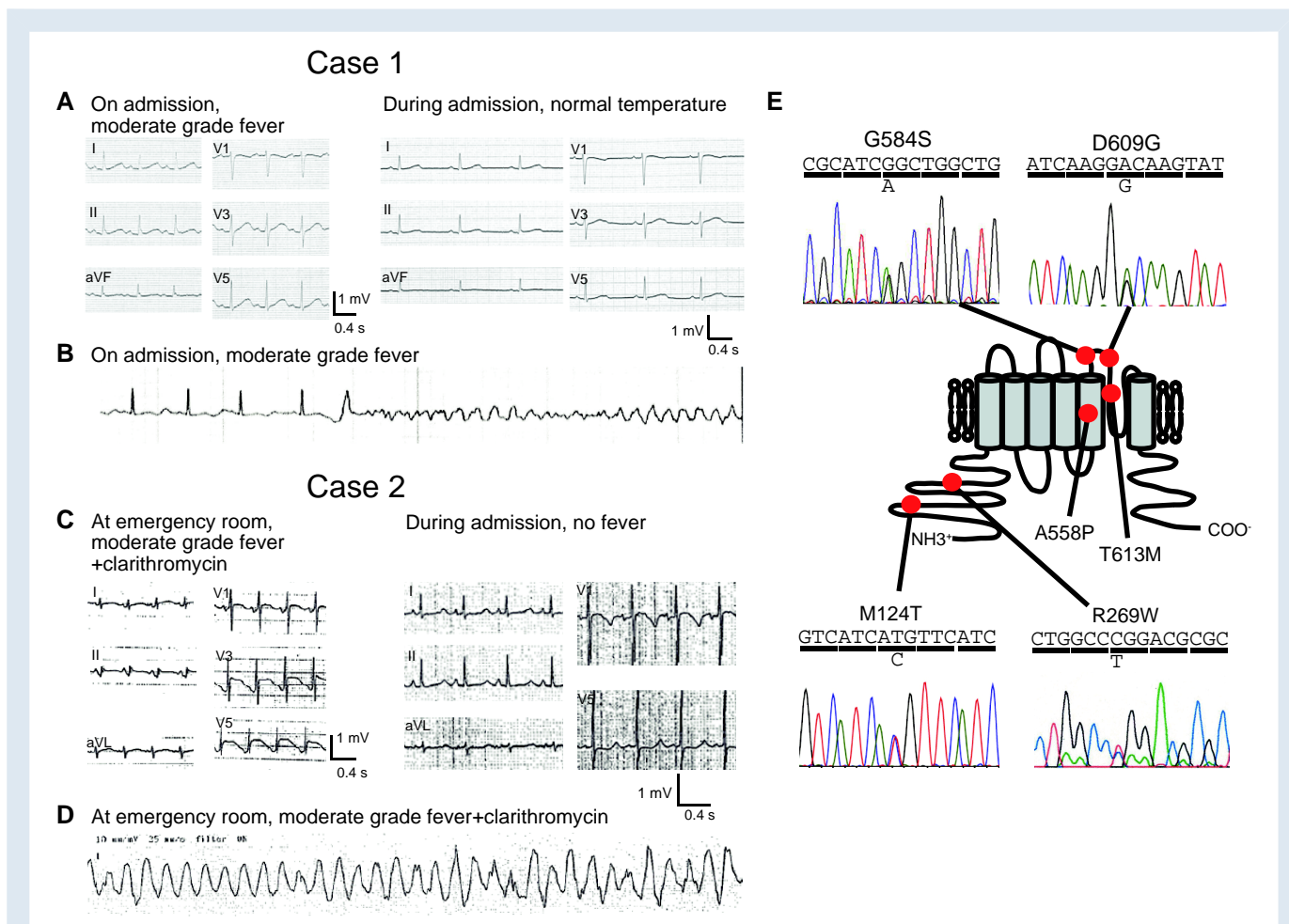
Figure 1 Electrocardiograms (ECGs) and location of *KCNH2* variants in patients with fever-induced long QT syndrome. (*A*) ECGs of Case 1 show a prolonged QTc (563 ms) during moderate grade fever and an almost normal QTc (444 ms) at normal temperature. (*B*) ECG obtained at the time of moderate grade fever shows torsade de pointes (TdP). (*C*) Case 2 has prolonged QTc intervals of 566 ms during moderate grade fever and 532 ms at normal temperature. (*D*) ECG obtained in the emergency room at the time of moderate grade fever shows TdP. (*E*) Illustrations of a Kv11.1 α-subunit with the cytoplasmic NH2- and COOH-terminus and six transmembrane segments. A558P, G584S, D609G, and T613M in the S5-pore region are associated with QT prolongation and TdP during fever. M124T and R269W are associated with QT prolongation but not with fever-induced QT prolongation and TdP.

S1A and S1B). The TCDs at 40 mV for the Kv11.1 channels showed that G584S, D609G, and T613M suppressed WT in a dominant-negative manner (see Supplementary material online, *Figure S1B* and Supplementary material online, *Table S3*).

We evaluated the kinetics and voltage dependence of Kv11.1 channel gating. Because D609G or T613M alone produced no functional channels, we studied co-expressed WT+D609G and WT+T613M, respectively. We assessed the voltage dependence of Kv11.1 activation using tail current analysis (see Supplementary material online, *Figure S2A* and Supplementary material online, *Table S4*). The potential at which half of the channels were activated ($V_{1/2}$) was -3.5 ± 0.8 mV for WT ($n = 102$). There were no significant differences in $V_{1/2}$ between all Kv11.1 channels. We assessed the voltage dependence of steady-state inactivation using a triple pulse voltage protocol (see Supplementary material online, *Figure S2B* and Supplementary material online, *Table S4*). The $V_{1/2}$ values for G584S, WT+D609G, and WT+T613M were -94.6 ± 4.8 mV ($n = 19$), -94.4 ± 3.0 mV ($n = 10$), and -105.4 ± 6.1 mV ($n = 9$), which were significantly shifted toward the negative direction compared to that of WT, M124T, and R269W (-76.0 ± 1.1 mV, $n = 64$; -75.2 ± 2.5 mV, $n = 17$; -79.5 ± 1.6 mV, $n = 18$) ($P < 0.01$). We

also determined the rate of channel inactivation using the triple pulse protocol (see Supplementary material online, *Figure S2C* and Supplementary material online, *Table S4*). The time constants of inactivation for M124T, G584S, WT+D609G, and WT+T613M showed significant attenuation compared with those for WT ($P < 0.01$).

Cellular electrophysiological properties of *KCNH2* wild-type and mutants at high temperature

We evaluated the effect of temperature on WT and mutant Kv11.1 channels to clarify the mechanisms of fever-induced QT prolongation and TdP. We measured the Kv11.1 currents using the whole-cell patch clamp technique at 35°C, which is equivalent to the physiological temperature in humans, and at 40°C, which mimics a febrile state in humans. *Figure 2A* shows representative tail current traces at 20 mV of the six different types of Kv11.1 channels at different recording temperatures. Tail current densities at 20 mV at 35°C for G584S, WT+D609G, and WT+T613M were significantly smaller than those for
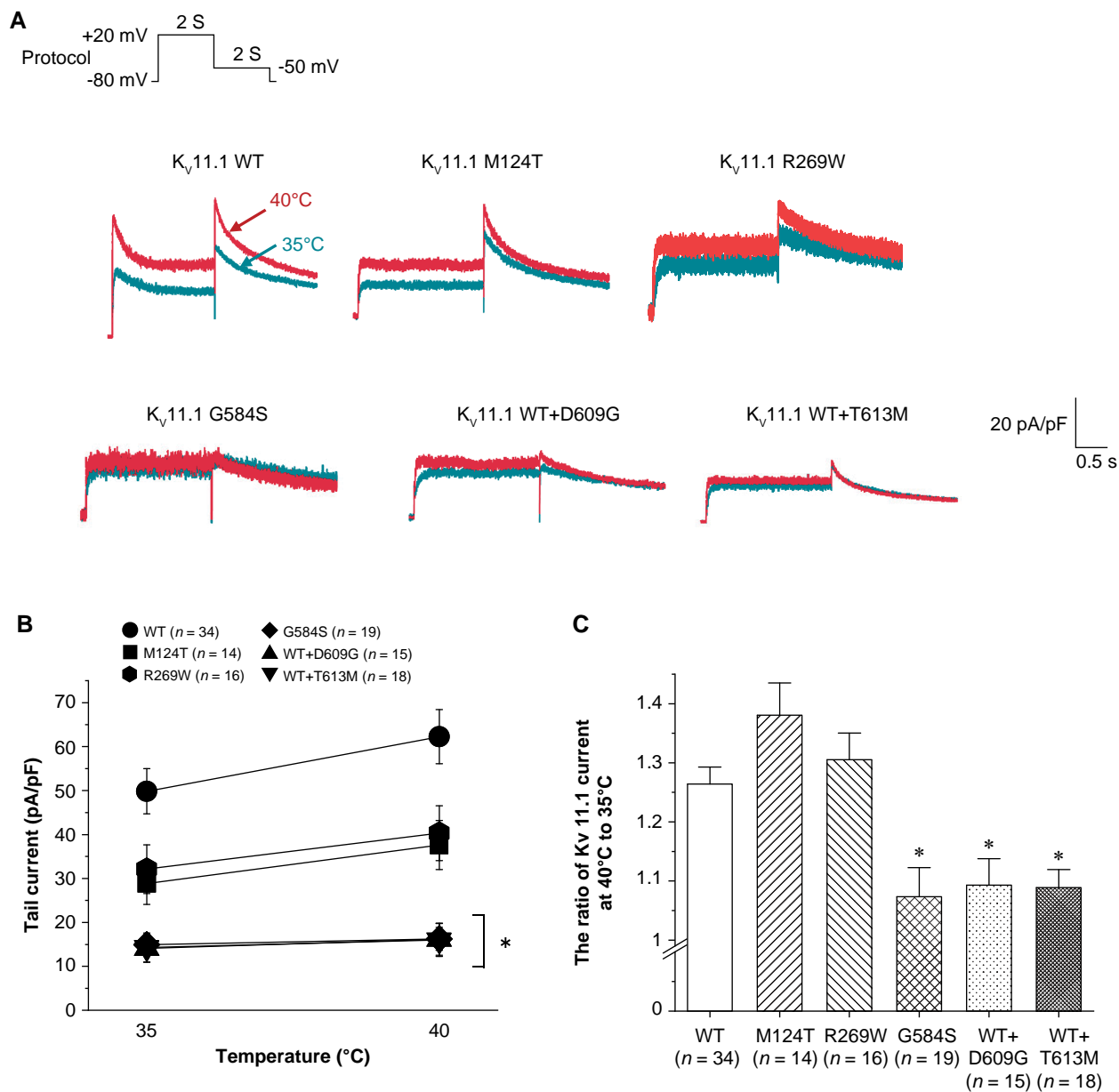
Figure 2 Temperature sensitivity of the Kv11.1 WT and mutant channels in CHO-K1 cells. (A) Representative currents recorded from CHO-K1 cells expressing WT alone, M124T alone, R269W alone, G584S alone, WT+D609G, and WT+T613M at 35°C and 40°C. The pulse protocol is shown in the inset. (B) Mean tail current densities (TCDs) at 20 mV for the six different types of Kv11.1 channels at 35°C and 40°C. * The temperature-dependent increases in TCD at 20 mV for G584S ($n = 19$), WT+D609G ($n = 15$), and WT+T613M ($n = 18$) were significantly lower with an increase in temperature from 35°C to 40°C than those for WT ($n = 34$), M124T ($n = 14$), and R269W ($n = 16$) ($P < 0.01$ by one-way ANOVA, followed by *post hoc* Tukey's test). (C) The ratio of Kv11.1 current at 40°C to 35°C for the six Kv11.1 channels. *$P < 0.01$ vs. WT, M124T, and R269W by one-way ANOVA, followed by *post hoc* Tukey's test.

WT, M124T, and R269W. The TCDs at 20 mV increased with a rise in temperature from 35°C to 40°C but the temperature-dependent increases in TCD at 20 mV for G584S, WT+D609G, and WT+T613M were significantly lower than those for WT, M124T, and R269W ($P < 0.01$) (*Figure 2A, 2B*, and *Table 1*). We assessed the ratio of Kv11.1 current at 40°C to 35°C (*Figure 2C*) to compare the magnitude of the thermal-dependent change in TCDs among the six Kv11.1 channels. The ratios for G584S (1.07 ± 0.05), WT+D609G (1.09 ± 0.04), and

WT+T613M (1.09 ± 0.03) were significantly lower than those for WT (1.26 ± 0.03), M124T (1.38 ± 0.05), R269W (1.31 ± 0.05) ($P < 0.01$ by one-way ANOVA, followed by a *post hoc* Tukey's test).

We then evaluated the kinetics and voltage dependence of Kv11.1 channel gating, including activation and inactivation at 35°C and 40°C. (see Supplementary material online, *Figure S3*). In all Kv11.1 channels, the steady-state activation curve at 40°C showed a marked negative shift compared to that at 35°C (*Figure 3A* and *Table 1*). The assessment of voltage

Table 1 Activation and inactivation parameters of the Kv11.1 channels at 35°C and 40°C

		35°C					
		WT	M124T	R269W	G584S	WT/D609G	WT/T613M
Tail current density at 20 mV	pA/pF	49.8 ± 5.1	28.9 ± 4.8	32.1 ± 5.5	14.9 ± 2.4	14.1 ± 3.1	14.3 ± 3.3
		($n = 34$)	($n = 14$)	($n = 16$)	($n = 19$)	($n = 15$)	($n = 18$)
Steady-state activation	$V_{1/2}$ (mV)	-19.1 ± 1.8	-17.2 ± 2.4	-14.4 ± 2.1	-18.9 ± 1.2	-20.2 ± 2.2	-20.1 ± 2.3
		($n = 13$)	($n = 13$)	($n = 13$)	($n = 13$)	($n = 13$)	($n = 13$)
	SF (mV)	6.6 ± 0.4	6.5 ± 0.4	6.7 ± 0.2	6.5 ± 0.4	5.8 ± 0.5	5.9 ± 0.4
		($n = 13$)	($n = 13$)	($n = 13$)	($n = 13$)	($n = 13$)	($n = 13$)
Steady-state inactivation	$V_{1/2}$ (mV)	-51.3 ± 2.6	-41.5 ± 3.6	-55.1 ± 3.0	-65.2 ± 3.8	-53.5 ± 2.8	-53.3 ± 2.0
		($n = 15$)	($n = 15$)	($n = 15$)	($n = 15$)	($n = 15$)	($n = 14$)
	SF (mV)	25.2 ± 1.4	25.1 ± 0.8	28.0 ± 1.2	24.3 ± 1.1	24.0 ± 1.6	22.3 ± 0.9
		($n = 15$)	($n = 15$)	($n = 15$)	($n = 15$)	($n = 15$)	($n = 14$)
		40°C					
		WT	M124T	R269W	G584S	D609G/WT	WT/T613M
Tail current density at 20 mV	pA/pF	62.3 ± 6.2*	37.6 ± 5.6*	40.3 ± 6.2*	16.3 ± 2.6	16.2 ± 3.7*	16.0 ± 3.7*
		($n = 34$)	($n = 14$)	($n = 16$)	($n = 19$)	($n = 15$)	($n = 18$)
Steady-state activation	$V_{1/2}$ (mV)	-30.3 ± 2.6*	-28.0 ± 1.6*	-25.0 ± 1.8*	-30.0 ± 1.5*	-30.3 ± 2.2*	-30.3 ± 3.1*
		($n = 13$)	($n = 13$)	($n = 13$)	($n = 13$)	($n = 13$)	($n = 13$)
	SF (mV)	5.1 ± 0.2*	5.5 ± 0.4*	6.3 ± 0.4	5.5 ± 0.4	5.3 ± 0.6	5.1 ± 0.4
		($n = 13$)	($n = 13$)	($n = 13$)	($n = 13$)	($n = 13$)	($n = 13$)
Steady-state inactivation	$V_{1/2}$ (mV)	-29.7 ± 2.5*	-15.6 ± 2.8*	-30.6 ± 3.5*	-57.3 ± 4.1*	-44.4 ± 2.8*	-46.2 ± 4.5
		($n = 15$)	($n = 15$)	($n = 15$)	($n = 15$)	($n = 15$)	($n = 14$)
	SF (mV)	19.4 ± 0.7*	20.0 ± 1.5*	24.4 ± 2.2	24.4 ± 1.5	25.0 ± 1.5	24.0 ± 2.7
		($n = 15$)	($n = 15$)	($n = 15$)	($n = 15$)	($n = 15$)	($n = 14$)

SF, Slope factor. *$P < 0.01$ vs. 35°C by paired *t*-test.

dependence of Kv11.1 activation showed that the $V_{1/2}$ values for WT and the five mutant channels were comparable at each recording temperature (*Table 1*). The differences in $V_{1/2}$ values for the steady-state activation curve at 35°C and 40°C were also comparable among all Kv11.1 channels (*Table 2*). *Figure 3B* shows the steady-state inactivation curves at 35°C and 40°C. As the temperature increased from 35°C to 40°C, the steady-state inactivation curves for all the five Kv11.1 channels except WT+T613M shifted significantly in a positive direction (*Figure 3B* and *Table 1*). The differences in $V_{1/2}$ values for the steady-state inactivation curve at 35°C and 40°C were significantly greater for WT, M124T, and R269W than for G584S, WT+D609G, and WT+T613M ($P < 0.01$). The differences were not significant among WT, M124T, and R269W (*Table 2*). *Figure 4*, Supplementary material online, *Figure S3C*, and Supplementary material online, *Table S5* show the rate of channel inactivation at 35°C and 40°C. As the temperature was increased from 35°C to 40°C, the time constants of inactivation for all Kv11.1 channels were significantly decreased. At 40°C, the time constants for inactivation of G584S, WT+D609G, and WT+T613M were not significantly different from that of WT.

Computer simulations of human ventricular action potentials and early afterdepolarization formation

The cellular electrophysiological study demonstrated that G584S, WT+D609G, and WT+T613M reduced temperature-dependent increases

in TCDs accompanied by enhancement of the steady-state inactivation at higher temperatures. To assess physiological implications of the alterations in channel properties by the mutations, we simulated EAD generations in the LQT2 cardiomyocytes using the Kurata *et al.* (human ventricular myocyte) model.[16] *Figure 5* shows the simulated effects of enhanced inactivation of the mutant Kv11.1 channel currents on APs of the M cells at 35, 37, and 40°C. G584S, WT+D609G, and WT+T613M, in contrast to WT, did not show temperature-dependent increases in I_{Kr} due to the smaller positive shift in the steady-state inactivation at 40°C. Consequently, repolarizations of APs were delayed by the smaller mutant channel currents, resulting in EAD formation at 40°C. In contrast, M124T, R269W, and WT exhibited significantly increased I_{Kr} during the febrile state, decreasing AP duration (*Figure 5*).

Discussion

This study investigated the clinical characteristics of patients with QT prolongation and TdP due to fever and harbored *KCNH2* G584S, D609G, or T613M in the Kv11.1 S5-pore region. We also characterized the temperature-dependent changes in the electrophysiological properties of these mutant Kv11.1 channels using heterologous expression systems. The cellular electrophysiological study and computer simulation study showed G584S, WT+D609G, and WT+T613M reduced temperature-dependent increases in TCDs
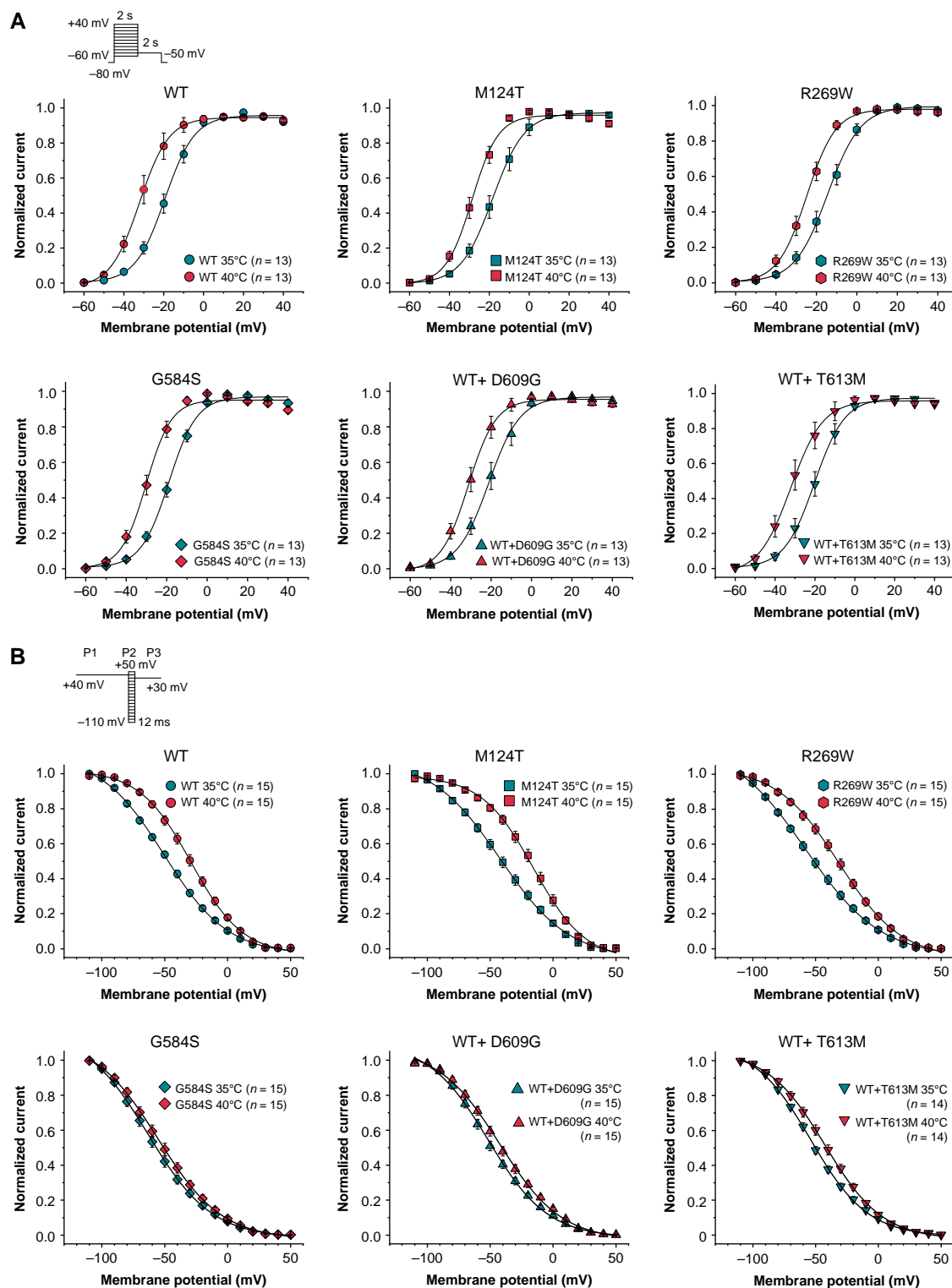
Figure 3 Temperature sensitivity of the voltage dependence of steady-state activation and inactivation in the Kv11.1 channels. (*A*) Summary of temperature-dependent shifts in the voltage dependence of steady-state activation for WT alone (*n* = 13), M124T alone (*n* = 13), R269W alone (*n* = 13), G584S alone (*n* = 13), WT+D609G (*n* = 13), and WT+T613M (*n* = 13) at 35°C (closed symbol) and 40°C (open symbol). The pulse protocol is shown in the inset. (*B*) Summary of temperature-dependent shifts in the voltage dependence of steady-state inactivation for WT alone (*n* = 15), M124T alone (*n* = 15), R269W alone (*n* = 15), G584S alone (*n* = 15), WT+D609G (*n* = 15), and WT+T613M (*n* = 14) at 35°C (closed symbol) and 40°C (open symbol). The pulse protocol is shown in the inset. The deactivation that occurred at more negative second pulse (P2) voltages of the triple pulse protocol was corrected. The peak current amplitude at the test potential was normalized and plotted against the prepulse potential. Curves represent the best fit by the Boltzmann function.

Table 2 Differences in $V_{1/2}$ of activation and inactivation curves at 35°c and 40°c

	WT	M124T	R269W	G584S	WT/D609G	WT/T613M
Differences in $V_{1/2}$ of activation curve	−11.2 ± 1.9	−10.1 ± 1.2	−10.5 ± 1.3	−10.8 ± 1.1	−10.1 ± 1.2	−10.2 ± 1.7
at 35°C and 40°C	(n = 13)	(n = 13)	(n = 13)	(n = 13)	(n = 13)	(n = 13)
Differences in $V_{1/2}$ of inactivation curve	21.6 ± 1.9*	25.9 ± 3.7[†]	24.4 ± 2.3[†]	7.9 ± 2.8	9.1 ± 2.0	7.0 ± 4.5
at 35°C and 40°C	(n = 15)	(n = 15)	(n = 15)	(n = 15)	(n = 15)	(n = 14)

*$P < 0.05$ or [†]$P < 0.01$ vs. G584S, WT/D609G, and WT/T613M by one-way ANOVA, followed by *post hoc* Tukey's test.
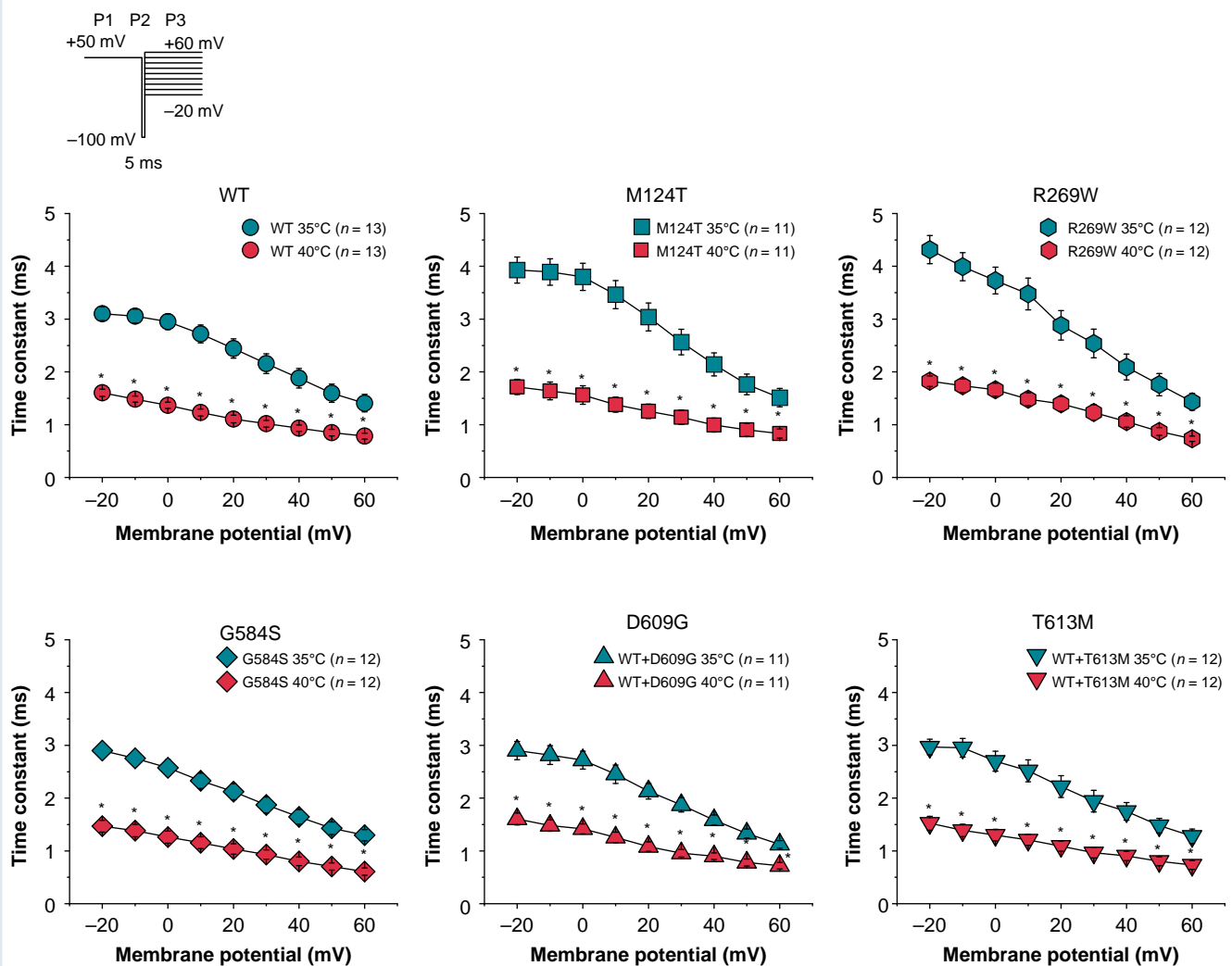

Figure 4 Temperature sensitivity of the rates of inactivation in Kv11.1 channels. Summary of temperature-dependent shifts in rates of inactivation for WT alone (n = 13), M124T alone (n = 11), R269W alone (n = 12), G584S alone (n = 12), WT+D609G (n = 11), and WT+T613M (n = 12) at 35°C (closed symbol) and 40°C (open symbol). The pulse protocol is shown in the inset. The inactivation rates at each potential were measured directly by fitting a single exponential function to the decay of the current. *$P < 0.01$ vs. 35°C by paired *t*-test.

through the reduced temperature-dependent depolarizing shift of steady-state inactivation. In contrast, as the temperature increased, WT, and M124T and R269W in the Kv11.1 N-terminus exhibited a greater increase in TCDs compared to G584S, WT+D609G, and WT+T613M. To our knowledge, this is the first demonstration of an association between the failure of temperature-dependent increases in I_{Kr} and enhanced steady-state inactivation of Kv11.1 channels at high temperatures.
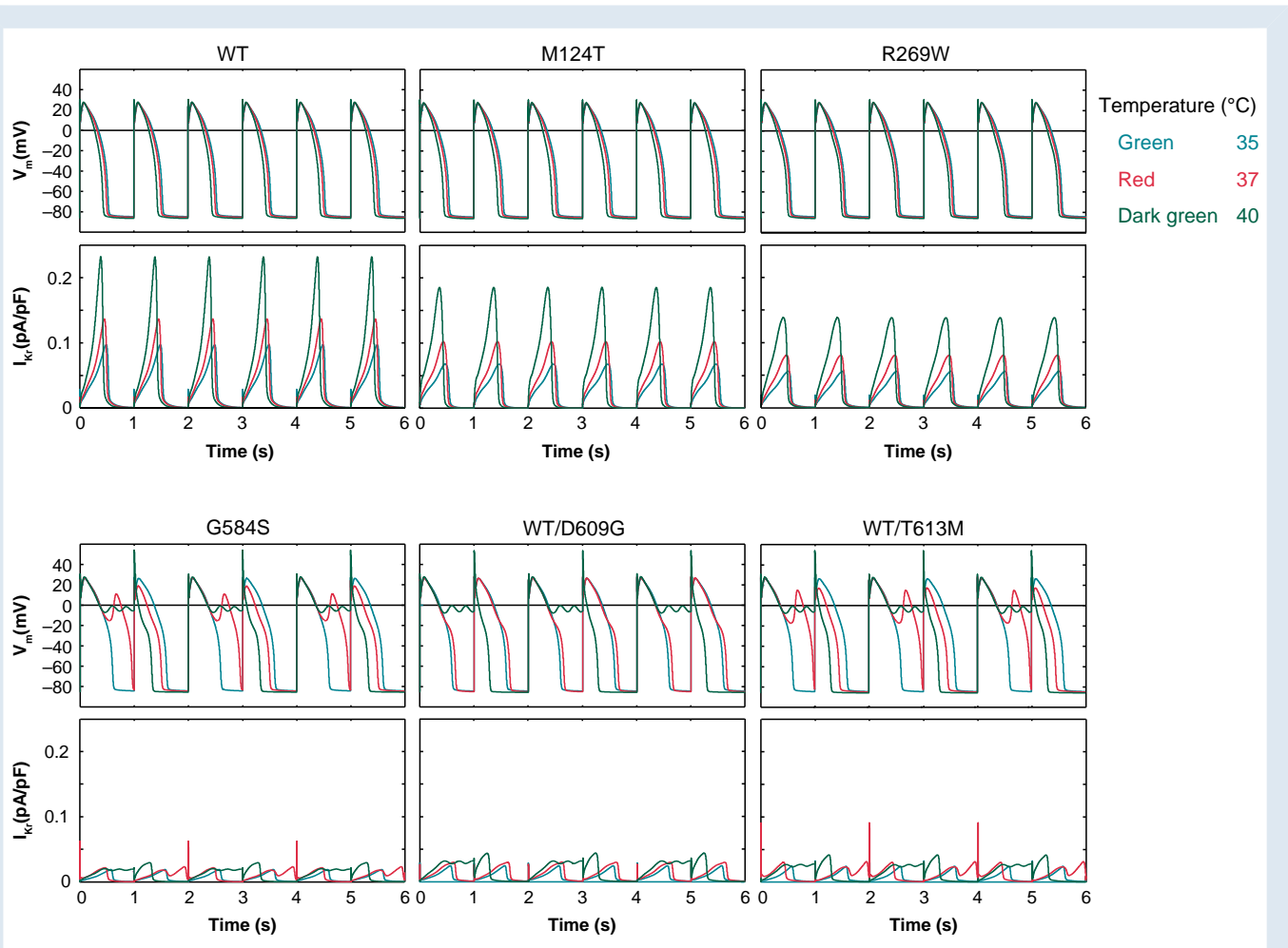
Figure 5 Simulated action potentials (APs) and I_{Kr} behaviors of the K05 models for the normal and type2 long QT syndrome cardiomyocytes (M cells) at 35, 37, and 40°C. The model cells with one of the *KCNH2* WT, M124T, R269W, G548S, WT+D609G, and WT+T613M channel currents were developed as described in the Methods section and Supplementary material online, *Table S2*. Model cells were paced at 1 Hz with 1-ms stimuli of 60 pA/pF for 30 min; the APs and I_{Kr} responses evoked by the last six stimuli are shown.

KCNH2 mutations identified in the patients with fever-induced QT prolongation and torsades de pointes

Cardiac events in patients with LQT2 are typically associated with emotional stress and sudden noise. Their association with fever has also been reported before, but only in a minority of cases.[4] Previous studies showed that A558P and T613M mutations in *KCNH2* genes were associated with fever-induced QT prolongation and ventricular tachyarrhythmia.[8,11] We identified patients with *KCNH2* mutations, namely, G584S and D609G, who developed marked QT prolongation and TdP at a relatively early phase (a few minutes to a few hours) of developing a low-grade fever (38°C or higher). The four mutations, G584S, D609G, T613M, and A558P, were located in the Kv11.1 S5-pore region. The Kv11.1 channel contains a long linker between the fifth transmembrane domain and the pore helix (S5P linker), which is important for the fast inactivation of this channel.[14] Previous studies showed that the S5P linker contributes to the voltage sensing for inactivation.[18]

Zhao *et al.*[19] reported a family with G584S with modest QT interval prolongation and six of 19 carriers exhibiting syncope. At the same time, there was no data regarding the types of triggers for the syncope.

They also showed that G584S traffic normally, and the mutant channels had abnormal inactivation gating. However, they did not describe changes in channel function with increasing temperature.

There are no reports on D609G other than our report. In Case 2, the proband had *KCNH2* D609G and *KCNQ1* D611Y. In the family members of Case 2, D611Y was identified in 12 members, and six of these subjects showed QT prolongation. *KCNH2* D609G was detected only in the proband, and no other family member presented TdP during fever. We previously reported that the current density of Kv7.1 D611Y was not significantly suppressed compared with that of Kv7.1 WT, but the rates of activation of the D611Y slowed compared with that of WT.[13] Therefore, we assumed that *KCNH2* D609G might be mainly associated with fever-induced QT prolongation and TdP. To clarify the role of the interaction between D609G-hERG and D611Y-Kv7.1 channels, we should also characterize the temperature-dependent changes in the electrophysiological properties of *KCNQ1* D611Y and conduct a simulation study to assess the physiological implications of alterations in both hERG and Kv7.1 channels.

There have been several reports on T613M. Huang *et al.*[20] reported that T613M showed a trafficking-deficient phenotype by chemiluminescence assay for surface expression of hERG protein, and T613M caused

a dominant-negative effect on Kv11.1 WT. They also showed no significant change of steady-state activation between WT and WT+T613M, and steady-state inactivation of WT+T613M was significantly shifted toward the negative direction compared to that of WT at room temperature (21°C to 23°C). These findings are consistent with our results, although they did not evaluate the temperature dependence of the channel function.

Electrophysiology of the mutant Kv11.1 channels at high temperature

Temperature can have acute and chronic effects on the Kv11.1 channel and hERG protein.[9,21] Previous studies have indicated that the acute effect is due to gating kinetics,[9] and the chronic effect is due to channel expression levels.[21] The present study focused on the former. We measured I_{Kr} currents at 35°C and 40°C at intervals of approximately 3 min. Vandenberg *et al.* showed that Kv11.1 channel currents that are heterologously expressed in CHO cells are markedly sensitive to changes in temperature; increasing temperature from 22°C to 37°C produced negative shifts in the voltage dependence of activation and positive shifts in the voltage dependence of inactivation.[9] Our results coincided with these findings. Clinically, Case 1 showed significant QT prolongation and TdP a few minutes after the onset of fever. In contrast, the duration of fever in Case 2 was unclear, but it might have been a few hours. Therefore, we speculate that the acute effects of temperature on the inactivation kinetics of Kv11.1 may influence the clinical phenotypes of both patients.

Amin *et al.*, for the first time, reported the acute electrophysiological effects of temperature on WT and WT+A558P currents; the normal increase in Kv11.1 WT current density at higher temperatures was reduced by the co-expression of A558P subunits, and A558P co-expressed with WT selectively accelerated the inactivation rates.[8] We also demonstrated that G584S, WT+D609G, and WT+T613M currents exhibit reduced temperature-dependent increases. In contrast to previously characterized *KCNH2* mutations identified in fever-induced LQTS, G584S alone could express functional channels without trafficking defect, which is a great advantage for analyzing the mechanisms of fever-induced QT prolongation and TdP. The difference from the results of Amin *et al.*'s study was that G584S, WT+D609G, and WT+T613M showed no difference in the inactivation rate at high temperatures compared to WT (*Figure 4*, Supplementary material online, *Table S5*); however, the three mutant channels showed significantly less change in steady-state inactivation with increasing temperature compared to WT, although Amin *et al.* did not evaluate the steady-state inactivation of the Kv11.1 current. The voltage dependence of Kv11.1 inactivation is an important contributor to determining AP duration.[22] Faster inactivation rates may not be the main reason for the prolongation of AP duration. We suggest the importance of smaller positive shifts in steady-state inactivation of Kv11.1 channels, which contributes to the failure of temperature-dependent increases in I_{Kr}.

Another interesting finding is that the M124T and R269W in the N-terminal domain yielded pronounced currents with rising temperature, similar to that for the WT channel, even though the TCDs at normothermia were smaller than that for WT. Because the steady-state activation kinetics of Kv11.1 channels were not significantly different for all tested channels, the differences in the increase of TCDs with increasing temperature between M124T and R269W in the N-terminal domain and G584S, WT+D609G, and WT+T613M in the S5-pore region are likely due to the differences in steady-state inactivation kinetics at high temperatures. These findings are consistent with the clinical phenotype, including that the *KCNH2* M124T carriers and R269W carriers had never experienced syncope during fever. We speculate that specific *KCNH2* mutations in the S5-pore region, which show impairments in the voltage dependence of inactivation with increasing temperature, may fail to increase I_{Kr} during fever.

Kiyosue *et al.* studied the acute effects of temperature on APs and membrane currents of guinea pig ventricular myocytes using a tight-seal whole-cell clamp technique.[6] They showed that the APD at 95% repolarization was 314 ± 83 ms at 24°C–25°C and 146 ± 33 ms at 33°C–34°C. They noted that the calcium current (I_{Ca}), the delayed rectifier potassium current (I_K), and the inwardly rectifying potassium current (I_{K1}) were sensitive to temperature, with Q_{10} (temperature coefficient) values of 2.3 ± 0.6 for I_{Ca}, 4.4 ± 1.2 for I_K tail current, and 1.5 ± 0.3 for I_{K1}. Thus, I_K is particularly sensitive to temperature and plays an important role in shortening the APD at high temperatures. These results suggest that patients with loss of I_{Kr} caused by *KCNH2* mutations may be prone to delayed cardiac repolarization and arrhythmias when they have fevers.[14] Our data support the hypothesis that patients with specific *KCNH2* mutations in the S5-pore region, which reduces the depolarizing shift of steady-state inactivation in a febrile state, may be at risk of fever-induced QT prolongation and TdP. For these patients, QTc interval monitoring and immediate treatment of fever with antipyretic drugs are highly recommended, as is the case for those diagnosed with Brugada syndrome.

Limitations

This study has several limitations. First, we assessed the functional consequences of *KCNH2* mutations using heterologous expression systems, not human cardiomyocytes. However, we believe these systems are useful to elucidate the mechanisms for channel dysfunction and how it leads to the arrhythmia phenotype because using these expression systems is a well-established method. Although experimental studies using induced pluripotent stem cells (iPS cells) may be more appropriate, recording stable APs in iPS cell-derived cardiomyocytes at varying temperatures is extremely challenging.

Second, we did not test whether *KCNH2* mutations in this study showed a trafficking-deficient phenotype, although the temperature can chronically affect channel expression levels. Zhao *et al.* studied the effects of febrile temperature culture on hERG channels in HEK 293 cells and on I_{Kr} in cardiomyocytes.[21] They showed that febrile temperature accelerates the degradation of hERG channels and chronically decreases hERG K^+ current. The data indicate that the specific *KCNH2* mutations may be at a higher risk of fever-induced QT prolongation and TdP in a chronic febrile state. On the other hand, in the present study, patients with fever-induced QT prolongation and TdP had cardiac events relatively early after the onset of high fever. Kv11.1 G584S, which has been reported to have normal trafficking, also showed reduced temperature-dependent increases in I_{Kr} and enhanced steady-state inactivation, as did WT+D609G and WT+T613M. These findings suggest the importance of the acute effect of temperature on the gating kinetics of the Kv11.1 channel.

Third, we did not conduct the patch clamp analysis and in silico simulations at 35°C and 40°C for co-expressed WT+G584S channels. Considering the heterotetrameric character of Kv11.1 channels, the presence of both WT and G584S subunits in the channels may change the results. In this study, we evaluated homotetrameric channels as much as possible because they can exhibit channel properties simply and strictly.

Fourth, we cannot exclude the possibility that fever-induced malignant arrhythmias with *KCNH2* G584S, WT/D609G, and WT/T613M result mainly from a large reduction in the I_{Kr} tail current at normal temperature rather than reduced temperature-dependent I_{Kr} increase due to enhanced Kv11.1 inactivation. It is currently difficult to distinguish between these two factors. To support our theory, we would need to identify and study a variant that notably reduces I_{Kr} tail current while maintaining a temperature-dependent I_{Kr} increase without fever-induced arrhythmias (EADs or TdPs), or conversely, a variant causing a small I_{Kr} tail current reduction but with a compromised temperature-dependent I_{Kr} increase and resulting fever-induced arrhythmias. There

might be a significant overlap between these situations. This issue should be addressed in future studies.

Finally, it should be noted that the patients with the *KCNH2* mutations in the S5-pore region might be affected by several risk factors, aside from a febrile state, which could cause QT prolongation and TdP, e.g. clarithromycin use in Case 2. Under these conditions of reduced repolarization reserve, reduced temperature-dependent increases in I_{Kr} during a febrile state could exacerbate QT prolongation and TdP.

Conclusions

We evaluated *KCNH2* mutations, namely, G584S, D609G, and T613M, in the S5-pore region identified in the patients with fever-induced QT prolongation and TdP. These mutations reduced temperature-dependent increases in I_{Kr} due to an enhanced Kv11.1 inactivation at a high temperature. Our findings indicate that the enhancement of inactivation of Kv11.1 channel during fever may contribute to QT prolongation and life-threatening arrhythmias in patients with specific *KCNH2* mutations in the S5-pore region.

Supplementary material

Supplementary material is available at *Europace* online.

Data availability

The data underlying this article are available in the article and in its online *supplementary material*.

Translational perspective

This study shows that some specific *KCNH2* mutations in the S5 pore region of the Kv11.1 channel reduce the temperature-dependent increase in TCDs due to an enhanced Kv11.1 inactivation at a high temperature. Namely, some patients with LQT2 and particular *KCNH2* mutations might be at risk of fever-induced QT prolongation and TdP. Understanding these mechanisms may contribute to the development of targeted therapies and management strategies for LQT2 patients with these specific mutations. Addressing the underlying mechanisms of fever-induced QT prolongation and TdP may potentially reduce the risk of life-threatening arrhythmias in these patients during febrile states.

References

1. Conte G, Scherr D, Lenarczyk R, Gandjbachkh E, Boule S, Spartalis MD *et al.* Diagnosis, family screening, and treatment of inherited arrhythmogenic diseases in Europe: results of the European Heart Rhythm Association Survey. *Europace* 2020;**22**:1904–10.
2. Mazzanti A, Trancuccio A, Kukavica D, Pagan E, Wang M, Mohsin M *et al.* Independent validation and clinical implications of the risk prediction model for long QT syndrome (1-2-3-LQTS-Risk): comment-Authors' reply. *Europace* 2022;**24**:698–9.
3. Wilde AAM, Amin AS, Postema PG. Diagnosis, management and therapeutic strategies for congenital long QT syndrome. *Heart* 2022;**108**:332–8.
4. Ravens U, Cerbai E. Role of potassium currents in cardiac arrhythmias. *Europace* 2008;**10**:1133–7.
5. Hayashi K, Shimizu M, Ino H, Yamaguchi M, Terai H, Hoshi N *et al.* Probucol aggravates long QT syndrome associated with a novel missense mutation M124T in the N-terminus of HERG. *Clin Sci (Lond)* 2004;**107**:175–82.
6. Kiyosue T, Arita M, Muramatsu H, Spindler AJ, Noble D. Ionic mechanisms of action potential prolongation at low temperature in guinea-pig ventricular myocytes. *J Physiol* 1993;**468**:85–106.
7. Nath S, Lynch C, 3rd, Whayne JG, Haines DE. Cellular electrophysiological effects of hyperthermia on isolated guinea pig papillary muscle. Implications for catheter ablation. *Circulation*. 1993; **88**(4 Pt 1):1826–31.
8. Amin AS, Herfst LJ, Delisle BP, Klemens CA, Rook MB, Bezzina CR *et al.* Fever-induced QTc prolongation and ventricular arrhythmias in individuals with type 2 congenital long QT syndrome. *J Clin Invest* 2008;**118**:2552–61.
9. Vandenberg JI, Varghese A, Lu Y, Bursill JA, Mahaut-Smith MP, Huang CL. Temperature dependence of human ether-a-go-go-related gene K^+ currents. *Am J Physiol Cell Physiol* 2006;**291**:C165–75.
10. Dumaine R, Towbin JA, Brugada P, Vatta M, Nesterenko DV, Nesterenko VV *et al.* Ionic mechanisms responsible for the electrocardiographic phenotype of the Brugada syndrome are temperature dependent. *Circ Res* 1999;**85**:803–9.
11. Shibata R, Ashizawa N, Komiya N, Fukae S, Nakao K, Seto S *et al.* Torsade de pointes triggered by high fever in patients with LQT2 syndrome (Japanese). *J Jpn Soc Int Med* 2009;**98**:1996–8.
12. Tange S, Imai M, Ui G, Kogure S, Ono Y, Kobayashi N *et al.* Tdp developed in a fever opportunity, once had a diagnosis of drug-induced LQT 7 years ago, showing KCNH2 mutant: a case report (Japanese). *Ther Res* 2012;**33**:1639–42.
13. Yamaguchi M, Shimizu M, Ino H, Terai H, Hayashi K, Kaneda T *et al.* Compound heterozygosity for mutations Asp611→Tyr in *KCNQ1* and Asp609→Gly in *KCNH2* associated with severe long QT syndrome. *Clin Sci (Lond* 2005;**108**:143–50.
14. Vandenberg JI, Perry MD, Perrin MJ, Mann SA, Ke Y, Hill AP. hERG K(+) channels: structure, function, and clinical significance. *Physiol Rev* 2012;**92**:1393–478.
15. Smith PL, Baukrowitz T, Yellen G. The inward rectification mechanism of the HERG cardiac potassium channel. *Nature* 1996;**379**:833–6.
16. Kurata Y, Hisatome I, Matsuda H, Shibamoto T. Dynamical mechanisms of pacemaker generation in IK1-downregulated human ventricular myocytes: insights from bifurcation analyses of a mathematical model. *Biophys J* 2005;**89**:2865–87.
17. O'Hara T, Virag L, Varro A, Rudy Y. Simulation of the undiseased human cardiac ventricular action potential: model formulation and experimental validation. *PLoS Comput Biol* 2011;**7**:e1002061.
18. Torres AM, Bansal PS, Sunde M, Clarke CE, Bursill JA, Smith DJ *et al.* Structure of the HERG K+ channel S5P extracellular linker: role of an amphipathic alpha-helix in C-type inactivation. *J Biol Chem* 2003;**278**:42136–48.
19. Zhao JT, Hill AP, Varghese A, Cooper AA, Swan H, Laitinen-Forsblom PJ *et al.* Not all hERG pore domain mutations have a severe phenotype: G584S has an inactivation gating defect with mild phenotype compared to G572S, which has a dominant negative trafficking defect and a severe phenotype. *J Cardiovasc Electrophysiol* 2009;**20**:923–30.
20. Huang FD, Chen J, Lin M, Keating MT, Sanguinetti MC. Long-QT syndrome-associated missense mutations in the pore helix of the HERG potassium channel. *Circulation* 2001;**104**:1071–5.
21. Zhao Y, Wang T, Guo J, Yang T, Li W, Koichopolos J *et al.* Febrile temperature facilitates hERG/IKr degradation through an altered K(+) dependence. *Heart Rhythm* 2016;**13**:2004–11.
22. Nakajima T, Furukawa T, Tanaka T, Katayama Y, Nagai R, Nakamura Y *et al.* Novel mechanism of HERG current suppression in LQT2: shift in voltage dependence of HERG inactivation. *Circ Res* 1998;**83**:415–22.